This is a post-peer-review, pre-copyedit version of an article published in Shape Memory and Superelasticity. The final authenticated version is available online at: https://doi.org/10.1007/s40830-020-00285-z

A short review on the effect of Cr on the fcc-hcp phase transition in Fe-Mn-based alloys

L.M. Guerrero [1,2,3], P. La Roca [1,2,3], F. Malamud [1,2,3], A. Baruj[1,2,3], M. Sade *[1,2,3]

[1] *Centro Atómico Bariloche (CNEA) Av. Bustillo 9500, 8400 Bariloche, Argentina*

[2]*Instituto Balseiro (Universidad Nacional de Cuyo-CNEA)*

[3]*CONICET, Argentina*

Abstract: The effect of Cr on the fcc-hcp martensitic transformation in the Fe-Mn-Cr system has been discussed considering different aspects: a) the relative phase stabilities, b) the magnetic order of the fcc phase, c) the structural parameters and volume change between fcc and hcp, d) the driving force of the martensitic transformation and relevant thermodynamics quantities, e) the thermal cycling behavior, and f) the pseudoelastic effect. Particularly, in this work it has been found that when Cr content increases, the effect of cycling on the energy barrier decreases. This may be explained by a small volume change, which could lead to a slighter introduction of plastic deformation during thermal cycling through the martensitic transition.

Key words: Fe-Mn-Cr, martensitic transitions, fcc-hcp transformation, shape memory alloys, cycling behavior, driving forces, volume change

Introduction

Fe-Mn-based systems have been widely studied in recent years due to the large number of technological applications derived from their outstanding mechanical properties. As presented by Chowdhury *et al*. [1], some of these applications are Hadfield steels (HS) primarily used in railroads, Twinning-induced plasticity / Transformation-induced plasticity (TWIP/TRIP) steels for the automotive industry, shape memory alloys (SMAs) useful as seismic dampers, and high entropy alloys (HEAs) that could be of use in cryogenics applications. Relevant mechanical properties depend on the chemical composition and on the thermomechanical history of the material and they are mainly due to the presence of a martensitic transformation.

In general, Fe-Mn-based shape memory alloys remain a low-cost option compared to systems such as NiTi-based alloys. The fcc-hcp martensitic transformation present in these systems is the basis of the shape memory effect (SME) which, in these alloys, is partial. In order to improve this effect, substituent elements such as Co, Si, Ni, Cr or some interstitials such as N and C are added. In addition, thermomechanical processes such as training and aus-forming treatments are also performed [2]. A good example of the combination of these modifications is found in the work of Wen *et al*. [3] in a cast and annealed polycrystalline Fe-20.2Mn-5.6Si-8.9Cr-5.0Ni steel that attains a tensile recovery strain of 7.6 %, which is an outstanding result.

The addition of Cr to Fe-Mn-based alloys usually aims at improving the corrosion resistance of the material. As Cr additions are large (5 wt.% or more), it is of interest to understand the role played by this element on the phase stability and mechanical properties of these alloys. In particular, the Fe-Mn-Cr ternary system inherits the martensitic transformation of the binary system. This first order transformation occurs between two crystalline phases, the parent

phase called austenite, which in this system is an fcc structure retained by quenching, and the product phase called martensite which is an hcp structure. The transformation is non-diffusive, and occurs by the cooperative displacement of atoms that produce a stacking fault every two atomic planes [4, 5]. This transformation can be induced by temperature changes or by the application of mechanical stress. It should be also mentioned that for Mn contents small enough, a bcc martensite might form [4]. This martensitic transition will not be considered in the present manuscript.

Recently, Fe-Mn-Cr-based alloys have made their entry into the so-called HEAs as introduced by M.D. Acciarri *et al*. [6] in a study of the effect of magnetic ordering on the relative phase stability in $Fe_{60-x}Mn_{30}Cr_{10}Co_X$ high entropy alloy. This system displays an excellent combination of ductility and mechanical resistance as reported by Z. Li *et al*. [7], comparable to $Fe_{20}Mn_{20}Ni_{20}Co_{20}Cr_{20}$ HEA system [8-10]. Recently, the FeMnNiCoCr HEA has also been compared to the CrCoNi medium-entropy alloy (MEA) [11, 12]; authors found that CrCoNi MEA has superior mechanical properties like ductility, toughness, and excellent cryogenic performance [13-15].

It is interesting to note that in the majority of polycrystalline Fe-Mn-Si-based SMAs alloys, where the maximum recovery strain has been achieved, Cr is present as a substituent element between 5 wt.% and 9 wt.% [3, 16-22]. And also, in the case of HEAs and MEAs with the best combination of ductility and mechanical resistance, the presence of Cr is found to be between 9 wt.% and 30 wt.% [7-15]. However, the effect of Cr has not been deeply discussed which makes it necessary to investigate the role of Cr on Fe-Mn-based systems for the design of new multicomponent alloys.

In this manuscript we present a review of the effect of Cr on several relevant physical magnitudes related to the fcc-hcp martensitic transition in Fe-Mn based alloys. A discussion based on recent results obtained by our research group is included and organized as a sequence of several topics. We analyze the effect of Cr on the martensitic transformation temperatures, critical magnetic ordering temperature of the austenite, lattice parameters, volume change, driving force of the martensitic transformation, thermal cycling and pseudoelasticity. Some of the results concerning the effect of Cr on thermal cycling through the fcc-hcp martensitic transformation are presented here as a first time, enriching the output of the manuscript.

Effect of Cr on the martensitic fcc-hcp transition temperatures

Until a few years ago, experimental information about the martensitic transformation temperatures (MTT) in the Fe-Mn-Cr system was scarce [23-25]. This transition occurs between the austenite phase, that in this system is fcc, and the martensite phase, which is hcp. Recently, a systematic study about the role of Cr on the fcc-hcp martensitic transition temperatures was published [25]. In this work, the authors studied the entire range of compositions where the fcc-hcp transformation takes place: between 2 wt.% and 12 wt.% Cr, and between 13 wt.% and 27 wt.% Mn. Critical temperatures for the start of the transformation from fcc to hcp (M_S) and from hcp to fcc (A_S) were measured by means of electrical resistivity and dilatometry. Authors found that by increasing Cr and Mn amounts, these temperatures tend to decrease [25].

Critical temperatures in Fe-Mn-based alloys depend on the thermomechanical history of the material [27]. In order to avoid these effects, measurements were performed in conditions where the microstructural modifications were negligible, that is, cast and homogenized alloys with large grain size containing very low densities of crystalline defects. Critical temperatures also depend on the para-antiferromagnetic transition of the austenite [27,28], which occurs at the Néel temperature (T_N). Considering this factor, three characteristic behaviors were found depending on whether the transformation occurs from a paramagnetic or antiferromagnetic austenite: $M_S>T_N$, $M_S\sim T_N$, and $M_S<T_N$. Figure 1 presents electrical resistivity measurements of Fe-Mn-Cr alloys under these three conditions. In the shown measured curves M_S is indicated by a small arrow and T_N by a dotted vertical line.

In Figure 1, curve (a) shows an alloy where $M_S>T_N$. The martensitic transformation starts in a paramagnetic state of the austenite. In cases like this, M_S is well described by Eq. 1 (Cr and Mn contents are expressed in wt.% and named W_{Cr} and W_{Mn}, respectively). This result is significant due to the possibility of modifying MTT by changing the chemical composition, thus allowing the design of alloys with special characteristics.

$$M_{S_{mod}}[K] = 524 - 6.12W_{Mn} - 4.05W_{Cr} \qquad \text{Eq. (1)}$$

(Please, place Fig. 1 about here)

Curve (b) shows the case where M_S is close to T_N. Both transitions, martensitic and magnetic, occur roughly simultaneously and compete with each other. Finally, curve (c) shows a situation where $M_S<T_N$. The transformation starts from an antiferromagnetic austenite; this condition causes the stabilization of this phase [29] hindering the fcc-hcp transformation. As a result, there is a drastic decrease in M_S. In some cases, in particular when T_N is clearly higher than M_S, the transformation might not occur. Under these conditions, Eq. 1 does not longer apply as it can be seen in Figure 2.

(Please, place Fig. 2 about here)

Eq. 1 results are represented as a solid line in Figure 2. The experimental data are in accordance with the proposed model when $M_S>T_N$, and the disagreement between experimental data and Eq. 1 is remarkable when $M_S < T_N$.

Effect of Cr on the para-antiferromagnetic transition temperatures

As mentioned before, the austenite phase has an antiferromagnetic transition at the Néel temperature. This magnetic ordering temperature depends on the chemical composition only [26,31,42] and, since it strongly affects the martensitic transformation, it is necessary to know how Cr and Mn additions affect T_N. In order to investigate that, Guerrero *et al*. [26] performed electrical resistivity and dilatometry measurements. They found that leaving Cr content

constant while increasing Mn content, T_N tends to increase. Conversely, by leaving Mn constant and increasing Cr content, the magnetic ordering temperature tends to decrease. They also proposed a phenomenological model that allows predicting T_N from the Cr and Mn content which even applies to the Fe-Mn system [30]. This model is shown below in Eq. 2. As well as for Eq. 1, Cr and Mn contents are expressed in wt.% and named W_{Cr} and W_{Mn}, respectively.

$$T_{N\,mod}[K] = 215 + (8.24 + 0.072W_{Cr})W_{Mn} - 3.64W_{Cr} - (0.043 + 0.0041W_{Cr})W_{Mn}{}^2 \qquad \text{Eq. (2)}$$

In Figure 3 it can be seen how Eq. 2 fits the experimental data reported in Refs. [26, 31]. It is noticed that T_N varies linearly respect to the Cr content and quadratically respect to the Mn. This model is also in agreement with the model presented by Huang [33] for the Fe-Mn system.

(Please, place Fig. 3 about here)

The stabilization of the fcc phase due to the para-antiferromagnetic transition [27, 30] and the possibility of controlling this transition by changing the chemical composition content, allow to obtain non-magnetic alloys. This type of alloy tends to have good mechanical properties at low temperatures [33] and, in this case, it could improve the shape memory effect.

Effect of Cr on the lattice parameters and on the volume change between fcc and hcp

Three different phases appear on quenched alloys in the Fe-Mn-Cr system depending on the chemical composition. These are: the austenite, or parent phase, having an fcc structure; the hcp martensite; and a bcc martensite that forms in alloys containing below 20 wt.% Mn [36]. The volume changes associated with martensitic transformations between these phases are usually large. The material tends to accommodate the transformation strain as plastic deformation, thus affecting other properties such as SME, TWIP or TRIP. In contrast, alloys where the volume changes associated to martensitic transformations are small display remarkable behaviors, like the pseudo-elastic properties found in Cu-based alloys [36,37], Ni-Ti-based alloys [38,39] and Fe-Mn-Al-Ni alloys [40,41]. It is then a significant question whether the volume change associated to the martensitic transformation of Fe-Mn-Cr alloys could be manipulated by controlling the chemical composition of these materials. Some limited information on the lattice parameters has been reported for the Fe-Mn-Cr system [42-44]. However, these studies used alloys that contained some impurities and other elements.

Recently, Malamud *et al*. [45] reported an experimental analysis about the effect of Cr and Mn on structural parameters of the three phases present in pure Fe-Mn-Cr alloys. Although the analysis of the bcc martensite is not aimed at this manuscript, it is interesting to notice that in the case of this structure, they found that the lattice parameter is not strongly affected by composition, as it was previously reported for the Fe-Mn system [46], and concluded that Cr has not a significant effect on the a_{bcc} lattice constant. In the cases of the fcc and hcp phases,

authors reported that lattice parameters depend linearly on the Mn content and tend to increase when Mn content increases. This result is in accordance with that reported for other Fe-Mn-based systems [34,42,46,47]. Lattice parameters tend to increase with the increment of Cr content, a variation which is well described by a quadratic expression. Equations that describe these behaviors with chemical composition are available in the published work [45].

From the calculated lattice parameters, it is possible to find the relative volume difference per atom between fcc and hcp phases $\left(\Delta V/V^{fcc}\right)$ as a function of the chemical composition. Considering the direct fcc to hcp transition we define ΔVas $\left(V^{hcp}-V^{fcc}\right)$, where V^{hcp} and V^{fcc} correspond to the volume per atom in each structure. Figure 4 shows the relative volume difference vs. Cr content for different amounts of Mn. This system exhibits a volume contraction when fcc-hcp martensitic transformation occurs, because the volume per atom in the fcc structure is larger than in hcp. In figure 4 the absolute value of the relative volume difference is plotted vs. Cr content.

(Please, place Fig. 4 about here)

In Figure 4, it can be seen that increasing Cr up to 6 wt.% the absolute value of the relative volume difference increases when Mn content increases, while for a content of 12 wt.% Cr, the same magnitude shows a decrease with the increase of Mn amount. This result opens up the possibility of finding Fe-Mn-Cr alloys where the volume change associated to the fcc/hcp martensitic transformation could be small. Under such circumstances, the phase transformation would only introduce a small amount of plastic deformation and, therefore, the reversibility of the transformation could be favored, thereby improving the overall SME.

This is an interesting result due to the possibility of controlling the volume change between these two phases through the chemical composition of the alloy. Recently, a validation of this prediction has been published in [48], where authors found a good agreement between the experimental and the predicted volume changes for two Fe-Mn-Cr alloys.

Effect of Cr on the driving force of the fcc-hcp transition

Kaufman and Cohen defined the driving force of the martensitic transformation as the difference between the Gibbs energies of each phase (ΔG), at the temperature at which the transformation occurs [49]. In the present manuscript the molar driving force corresponding to the direct fcc-hcp transition ΔG_m is defined as $\left(G_m^{hcp}-G_m^{fcc}\right)$. In this work we will apply the concept of driving force only for the direct fcc-hcp transition. Due to this reason we will not indicate the transition when writing (ΔG). Recently, a work about the experimental determination of the driving force of the fcc-hcp martensitic transformation in Fe-Mn-Cr system was published [50]. In this paper, authors used the definition of T_0 as the temperature at which both Gibbs energies of fcc and hcp structures are equal [49] and some approximations to obtain an expression that would allow to determine the driving force of the transformation from experimental measurements. The authors considered that T_0 depends on M_S and A_S temperatures [27, 29], and that in order to obtain experimental values of the driving force, M_S should be higher than T_N [28, 30]. For this purpose a thermodynamic procedure was developed in ref [50]: The difference of Gibbs free energy between fcc and hcp at constant

pressure and temperature can be written as $\Delta G|_T = \Delta H|_T - T\Delta S|_T$, where $\Delta H|_T$ is the enthalpy change at temperature T and $\Delta S|_T$ is the corresponding entropy change at the same temperature. At $T = T_0$, we have $\Delta G|_{T=T_0} = 0$ and thus, $\Delta H|_{T_0} = T_0 \Delta S|_{T_0}$. Close to the transformation temperature the entropy change can be approximated as $\Delta S|_T = \Delta S|_{T_0} = \frac{\Delta H|_{T_0}}{T_0}$. This requires a small difference between specific heats of each phase in the temperature interval from T to To. Additionally, the enthalpy change can be also regarded as independent of temperature, i.e., $\Delta H|_{T_0} = \Delta H|_T$, if the same requirement on the specific heats is also fulfilled. Using both approximations the difference between Gibbs free energies corresponding to fcc and hcp structures can be written as $\Delta G|_T = \Delta H|_T - T\frac{\Delta H|_{T_0}}{T_0} = \frac{T_0 \Delta H|_T - T\Delta H|_{T_0}}{T_0}$ obtaining [50]:

$\Delta G_m\|_T = \frac{\Delta H_m\|_{T_0}(T_0 - T)}{T_0}$	Eq. (3)

In Eq. 3 the subinde "m" is added to ΔG and ΔH, to emphasize that these magnitudes are extensive, being "m" an indication that we use here molar quantities.

One remarkable point is that the required small difference in specific heat between fcc and hcp phases was experimentally verified. From modulated differential scanning calorimetry (MDSC) measurements, the specific heat difference between the involved phases has been determined, resulting in approximately 2.5 % of the C_P values [50]. In practice, the mentioned difference in C_P values between austenite and martensite can be taken as negligible.

Under the mentioned conditions, all the magnitudes in the right member of Eq. 3 can be determined from experimental measurements. As an example, T_0 is obtained as the average between M_S and A_S, critical transition temperatures , which have been determined by electrical resistivity and dilatometry measurements. The molar enthalpy change ($\Delta H_m|_{T_0}$) depends on the transformed fraction of the alloys (that can be determined by means of dilatometry and X-Rays diffraction) and on the heat exchanged during transformation (measured with Differential Scanning Calorimetry, DSC).

Experimentally determined driving forces for the Fe-Mn-Cr system at the transformation temperatures are presented in Figure 5 as a function of Cr content for different Mn amounts. The driving force depends on composition through the martensitic transformation temperatures, since it has been shown that the enthalpy change between fcc and hcp can be considered independent on composition in the composition range where this martensitic transition takes place [50].

(Please, place Fig. 5 about here)

As it can be seen in Figure 5, the driving force shows a stronger dependency on the Mn content than on the Cr amount, but the absolute value increases when both of the

components increase. The values reported in this work, 165 J/mol < ΔG_m< 240 J/mol, are within the range of the values found in the literature for other Fe-Mn-based systems [28, 52-54].

According to the Olson and Cohen model [55] for the nucleation of hcp martensite from an fcc austenite, the driving force $\left(\Delta G_m^{fcc-hcp}\right)$ is the energy necessary for the transformation to start. This implies that it must be enough to overcome the barriers that oppose the transformation [55-57]. These barriers comprise the surface energy (E^{sur}) necessary to form the interfaces between fcc and hcp phases, and the elastic strain energy (E_m^{st}) necessary for the transformation to begin, also in J/mol. These conditions are expressed below in Eq. 4.

$$\tau(n) = n\rho\left(\Delta G_m^{fcc-hcp} + E_m^{st}\right) + E^{sur} \qquad \text{Eq. (4)}$$

Here, $\tau(n)$ is the energy change when a nucleus of martensite is produced, and depends on the number of planes in the nucleus (n). ρ is the atomic density of the basal plane in mol/m^2. The surface energy (E^{sur}) is about 14 mJ/m^2 [29,52,53,58]. Both members of Eq. 4 should be equal to 0 when the transformation starts, i.e at temperature equal to M_S and when n corresponds to the critical nucleus.

The strain energy term (E_m^{st}) of the Fe-Mn-Cr system was determined from experimental lattice parameters and relative volume difference during martensitic transformation as reported in Ref. [45]. In that work, authors found that Mn content does not produce a significant effect on strain energy. However, they observed that this energy decreases when the content of Cr increases. This behavior can be seen in Figure 6.

(Please, place Fig. 6 about here)

Figure 6 shows the strain energy obtained as function of the Cr content leaving the Mn content constant. As the amount of Cr increases, the elastic strain energy tends to decrease which could also facilitate the reversibility of the transformation, thus enhancing the SME of these alloys.

By making $n = 2$ in Eq. 4, the stacking fault energy (SFE) could be obtained. This is very interesting due to the possibility of combining Eq. 3 and 4, and obtaining an expression that allows determining the SFE as a function of temperature, as shown in Ref. [50]:

$$SFE(T) = 2\rho\left(\frac{{\Delta H_m}^{fcc-hcp}\big|_T (T_0 - T)}{T_0} + E_m^{st}\right) + E^{sur} \qquad \text{Eq. (5)}$$

Eq. 5 describes a linear dependence of SFE vs. temperature, and varies with chemical composition trough T_0; all the terms can be obtained from experimental measurements.

Effect of Cr on the thermal cycling between fcc and hcp

To the best of our knowledge, only a few works about thermal cycling through the martensitic transformation in Fe-Mn-Cr alloys have been published [24, 25, 59]. M. Sade *et al.*

[25] have found that thermal hysteresis enlarges after thermal cycling, because A_S increases while M_S decreases as cycling proceeds. They also reported that with few thermal cycles it is possible to reach an asymptotic state, which is different from previous findings in Fe-Mn-based systems [53, 60]. TEM observations in cycled samples indicate the presence of a large stacking faults density, which could favor the SME [61], and a large dislocations density. The accumulation of plastic deformation is due to the considerable volume change between fcc-hcp phases during the martensitic transformation, as it is the case for the Fe-Mn system [46] and for the Fe-Mn-Cr system [48].

From the information published recently by our group on this alloy [50], we can perform an analysis of thermal cycling from the point of view of thermodynamics of the nucleation of hcp martensite from fcc austenite matrix, using the expression shown in Eq. 3.

Five Fe-Mn-Cr alloys were made from commercial pure metals in an arc furnace under Ar atmosphere, then the specimens were homogenized at 1273 K in quartz capsules for 48 h under Ar atmosphere, and they were quenched in water at room temperature. After that, electrical resistivity samples were cut by spark-cutter, then polished and heat-treated in individual quartz capsules at 1273 K for 1 h under Ar atmosphere, and finally water quenched. Chemical composition of the alloys was determined by neutron activation analysis at RA-6 experimental nuclear reactor at Centro Atómico Bariloche, being these results shown in Table 1. Thermal cycling was made in a homemade electrical resistivity equipment, as described in Ref. [25], between $T<M_F$ (martensite finish) and $T>A_F$ (austenite finish).

(Please, place Table 1 here)

An example of an electrical resistivity measurement is shown in Figure 7. Here sample A was subjected to 11 thermal cycles and it can be seen that M_S decreases between cycles 1 ($M_S^{N=1}$) and 11 ($M_S^{N=11}$). It is also noticed that the last two cycles overlap, which is consistent with the results reported before in Ref. [25].

(Please, place Fig. 7 about here)

Also in Ref. [25] authors report that M_S strongly decreases due mainly to the dislocation introduction during thermal cycling. These dislocations make thermal martensitic transformation difficult, in view of the fact that the alloy must be further cooled in order to have sufficient driving force to enable the phase transformation.

Combining the Olson and Cohen model with Eq. 4, and using the driving force calculated with Eq. 3 (Table 1), we can relate the change in M_S with the additional driving force necessary to overcome the new barrier, which in this case mainly corresponds to the density of dislocations

introduced during thermal cycling. In order to use the ΔG_m expression from Eq. 3, it is a necessary condition that T_N<M_S. As it can be seen in Table 1, all selected alloys meet this condition.

For the first cycle, at M_S we have the following condition:

$$T = M_S^{N=1} \rightarrow \Delta G_m^{N=1} = \frac{\Delta H_m (T_0 - M_S^{N=1})}{T_0} \qquad \text{Eq. (6)}$$

And, for the next cycle, the condition at the new M_S is:

$$T = M_S^{N=2} \rightarrow \Delta G_m^{N=2} = \frac{\Delta H_m (T_0 - M_S^{N=2})}{T_0} \qquad \text{Eq. (7)}$$

Where $M_S^{N=2}$ corresponds to the measured M_S at transformation number $N = 2$. So, the difference of the driving force between the first and the next cycle is:

$$\Delta(\Delta G_m) = \Delta G_m^{N=1} - \Delta G_m^{N=2} = \frac{-\Delta H_m (M_S^{N=1} - M_S^{N=2})}{T_0} \qquad \text{Eq. (8)}$$

This difference of driving force is related to the increment in the barrier that opposes the transformation, as follows,

$$\tau_1(n) = 0 = n\rho(\Delta G_m^{N=1} + E_m^{st}) + E^{sur} \qquad \text{Eq. (9)}$$

For the next cycle, the condition for the martensitic transformation to start is:

$$\tau_2(n) = 0 = n\rho\left(\Delta G_m^{N=2} + E_m^{N=2,d} + E_m^{st}\right) + E^{sur} \qquad \text{Eq. (10)}$$

Where $E_m^{N,d}$ is the increase in the molar energy barrier, being N the number of performed cycles and we use the superscript *d* to emphasize that the origin of this term is related to the introduced dislocations. This energy is considered negligible at $N = 1$ and depends on the number of cycles. Due to this reason $E_m^{N,d}$ is not present in Eq. 9. The difference between the right members of energy balances of the first and the second cycle, in Eq. 9 and 10 should equal 0 as shown in the following equation:

$$0 = n\rho\left(\Delta G_m^{N=1} - \left(\Delta G_m^{N=2} + E_m^{N,d}\right)\right) \qquad \text{Eq. (11)}$$

It is then deduced that:

$$\Delta G_m^{N=1} - \Delta G_m^{N=2} = E_m^{N=2,d} \qquad \text{Eq. (12)}$$

In order to obtain Eq. 12, we make the approximation that the number of planes (n) in the critical nucleus, the elastic strain energy (E_m^{st}) and the surface energy (E^{sur}), do not change after a few thermally induced transformations. This is plausible since the main change during thermal cycling is the introduction of dislocations

Combining Eq. 8 and 12, we have a new expression that relates $E_m^{N,d}$ with the variation of ΔG_m^N, which depends on the variation of M_S:

$$\Delta^N(\Delta G_m) = \Delta G_m^{N=1} - \Delta G_m^N = \frac{-\Delta H_m (M_S^{N=1} - M_S^N)}{T_0} = E_m^{N,d} \qquad \text{Eq. (13)}$$

The ratio between $E_m^{N,d}$ and $\Delta G_m^{N=1}$ with the cycle number is shown in Figure 8, where it can be seen the effect of Cr for a constant Mn content of 20 Wt.%.

(Please, place Fig. 8 about here)

In Figure 8, it is observed that at a higher amount of Cr, leaving the content of Mn constant, the ratio $\left|E_m^{N,d}/\Delta G_m^{N=1}\right|$ tends to be smaller, that is, the alloy is less susceptible to thermal cycling. This means that the energy barrier increases less with cycling when Cr content increases. This reinforces the idea that by increasing Cr content, a stable condition is reached rapidly, that is, after few thermal cycles an asymptotic state is reached after a few cycles.

Now, if we compare two different Mn contents, with different amounts of Cr, we have the curves shown in Figure 9, where the number close to each curve is the volume change related to the fcc-hcp martensitic transformation.

(Please, place Fig. 9 about here)

The general trend is that the effect of thermal cycling through the fcc-hcp transformation is less strong as the volume change between both phases decreases. Additionally it is already known that the relative volume change between austenite and hcp decreases as Mn and Cr contents increase. Particularly the increase of Cr also decreases the strain energy introduced by the model of Olson and Cohen. It is then remarkable that the effect of Cr seems to have several positive consequences like the decrease in the energy barrier to transform and a possible increase of the reversibility in the shape memory effect due to its effect on the volume change.

Presence of pseudoelasticity in Fe-Mn-Si-Cr alloys

Pseudoelasticity describes the ability of a material to recover its original shape beyond the elastic limit during unloading, without a retransformation heating step [62]. In the work of Baruj *et al*. [63], they observed a moderate pseudoelastic behavior between 90 °C and 100 °C during tensile tests, and about 80 % of the maximum deformation was recovered at a strain level of 0.3 %. They also found that the cycles were not completely closed due to stress-induced martensite and plastic deformation was introduced during each test. From TEM

observations, they suggested that this pseudoelasticity may be due to the presence and creation of stacking faults, and the movement of their associated partial dislocations.

In several studies where the presence of pseudoelasticity in the Fe-Mn-Si-Cr system is reported [63-69], the Cr content is between 4 wt.% and 9 wt.%, which is within the range of the alloys analyzed in the present work. The presence of this element is generally related to its anticorrosive effects [70], but the effect of Cr on pseudoelasticity has not been analyzed. As mentioned earlier in this work, it could be said that Cr might have a beneficial effect on this property, since it has the effect of reducing the volume change.

Final comments and conclusions

In the present work, the role of Cr in different aspects of the fcc-hcp martensitic transformation in the Fe-Mn-Cr system has been discussed, aiming at improving the alloys design with specific properties. The most relevant results are listed below.

- The addition of Cr tends to decrease the fcc-hcp martensitic transformation temperatures (M_S and A_S), which produces a stabilizing effect of the austenite phase.
- The increment on Cr content also decreases the antiferromagnetic ordering temperature (T_N), which has the opposite effect, i.e., it decreases the stability of austenite.
- Cr addition causes the lattice parameters (a_{fcc}, a_{hcp}, c_{hcp}) to increase.
- The increment in Cr content tends to decrease the volume change during fcc-hcp martensitic transformation, which has the effect of decreasing the elastic strain energy.
- The driving force of the fcc-hcp martensitic transition is also affected by Cr content, tending to decrease with the increase of Cr amount.
- When Cr content increases, the effect of cycling on the energy barrier decreases. This may be due to the small volume change between fcc and hcp, which might lead to a lower introduction of plastic deformation.
- Cr content can improve pseudoelasticity, because this element stabilizes the austenite phase and reduces the volume change.
- Finally and besides the positive effects of Cr on corrosion resistance, we can affirm that this element plays remarkable roles on several of the most significant properties related to the martensitic fcc-hcp transition in Fe-Mn based alloys.

Acknowledgments

It is a pleasure to contribute to this special issue in honor to the distinguished trajectory of Professor Gunther Eggeler in the field oh Shape Memory Alloys. It has been a pleasure to share years of fruitful collaboration and warm friendship with him.

Funding

The authors acknowledge the financial support from ANPCyT (PICT-2017-2198), CONICET (PIP 2015-112-201501-00521), CONICET (PIP 2017–2019 GI 0634), ANPCyT (PICT-2017-4518), and Universidad Nacional de Cuyo (06/C516 and 06/C588). The help of E. Aburto and M. Isla with quartz capsules is gratefully acknowledged.

References

[1] Chowdhury P., Canadinc D., Sehitoglu H.: On deformation behavior of Fe-Mn based structural alloys, Mater. Sci. Eng. R 122 (2017) 1-28

[2] Peng H., Chen J., Wang Y. and Wen Y.: Key factor achieving large recovery strains in policrystalline Fe-Mn-Si-based shape memory alloys: A review, Adv. Eng. Mater. 2017, 1700741

[3] Wen Y.H., Peng H.B., Raabe D., Gutierrez-Urrutia I., Chen J. and Du Y.Y.: Large recovery strain in Fe-Mn-Si-based shape memory steels obtained by engineering annealing twin boundaries, Nat. Commun. (2014) 5, 4964

[4] La Roca P., Baruj A., Sade M.: Shape-memory effect and pseudoelasticity in Fe-Mn-Based alloys, Shap. Mem. Superelasticity (2017) 3:37-48

[5] Chowdhury P., Sehitoglu H.: Deformation physics of shape memory allos – Fundamentals at atomistic frontier, Prog. Mater. Sci. 88 (2017) 49-88

[6] Acciarri M.D., La Roca P., Guerrero L.M., Baruj A., Curiale J., Sade M.: Effect of FCC anti-ferromagnetic ordering on the stability of phases in $Fe_{60-X}Mn_{30}Cr_{10}Co_X$ high entropy alloys, J. Alloy. Compd. 823 (2020) 153845

[7] Li Z., Pradeep K.G., Raabe D.: Metastable high-entropy dual-phase alloys overcome the strength-ductility trade-of, Nature 354 (2016)

[8] Gludovatz B., Hohenwarter A., Catoor D., Chang E.H., George E.P., Ritchieet R.O.: A fracture-resistance hihg-entropy alloy for cryogenic applications, Science 345, 1153-1158 (2014)

[9] Otto F., Dlouhý A., Somsen Ch., Bei H., Eggeler G., George E.P.: The influences of temperature and microstructure on the tensile properties of CoCrFeMnNi high-entropy alloy. Acta Mater. 61, 5743-5755 (2013)

[10] Laplanche G., Kostka A., Horst O.M., Eggeler G., George E.P.: Microstructure evaluation and critical stress for twinning in the CrMnFeCoNi high-entropy alloy, Acta Mater. 118 (2016) 152-163

[11] Laplanche G., Kostka A., Reinhart C., Hunfeld J., Eggeler G., George E.P.: Reasons for the superior mechanical properties of medium-entropy CrCoNi compared to high-entropy CrMnFeCoNi, Acta Mater. 128 (2017) 292-303

[12] Schneider M., George E.P., Manescau T.J., Záležák T., Hunfeld J., Dlouhý A., Eggeler G., Laplanche G.: Analysis of strengthening due to grain boundaries and annealing twin boundaries in the CoCrNi medium-entropy alloy, Int. J. Plast. (2020) Vol. 124 155-169

[13] Q. Ding, X. Fu, D. Chen, H. Bei, B. Gludovatz, J. Li, Z. Zhang, E. P. George Q. Yu T. Zhu, R. O.Ritchie, "Real-time nanoscale observation of deformation mechanisms in CrCoNi-based medium- to high-entropy alloys at cryogenic temperatures", Materials Today, 25, May 2019, Pages 21-27

[14] W. Woo, J. S. Jeong, D.-K. Kim, C. M. Lee, S.-H. Choi, J.-Y. Suh, S. Y. Lee, S. Harjo & T. Kawasaki, "Stacking Fault Energy Analyses of Additively Manufactured Stainless Steel

316L and CrCoNi Medium Entropy Alloy Using In Situ Neutron Diffraction", Scientific Reports volume 10, Article number: 1350 (2020)

[15] E. Slone, J. Miao, E. P. George, M.J. Mills "Achieving ultra-high strength and ductility in equiatomic CrCoNi with partially recrystallized microstructures", Acta Materialia, 165, 2019, Pages 496-507

[16] Kajiwara S., Liu D., Kikuchi T., Shinya N.: Remarkable improvement of shape memory effect in Fe-Mn-Si based shape memory alloys by producing NbC precipitates, Scr. Mater. (2001) 44, 2809

[17] Dunne D.P., Li H.: The mechanism of thermomechanical training of a newly developed Fe-Mn-Si-Cr-Cu shape memory alloy. J. Phys. IV (1995) 5, C8

[18] Baruj A., Troiani H.: The effect of pre-rolling Fe–Mn–Si-based shape memory alloys: Mechanical properties and transmission electron microcopy examination. Mater. Sci. Eng. A (2008) 481-482, 574

[19] Baruj A., Kikuchi T., Kajiwara S., Shinya N.: Improvement of shape memory properties of NbC containing Fe–Mn–Si based shape memory alloys by simple thermomechanical treatments. Mater. Sci. Eng. A (2004) 378, 333

[20] Peng H.B., Wen Y.H., Liu G., Wang C.P., Li N.: A Role of α' Martensite Introduced by Thermo-Mechanical Treatment in Improving Shape Memory Effect of an Fe-Mn-Si-Cr-Ni Alloy. Adv. Eng. Mater. (2011) 13, 388

[21] Stanford N., Dunne D.P.: Thermo-mechanical processing and the shape memory effect in an Fe–Mn–Si-based shape memory alloy. Mater. Sci. Eng. A (2006) 422, 352

[22] Wang D., Liu D., Dong Z., Liu W., Chen J.: Improvement of shape memory effect by ausforming in Fe–28Mn–6Si–5Cr alloy. Mater. Sci. Eng. A (2001) 315, 174

[23] Mertinger V., Nagy E., Benke M., Tranta F.: Characteristics of martensitic transformations induced by uni-axial tensile tests in a FeMnCr steel. Mater Sci Forum 812 (2015) 161-166

[24] Troiani H.E., Sade M., Bertolino G., Baruj A.: Martensitic transformation temperatures and microstructural features of FeMnCr Alloys. Proc Esomat 2009, 06002 (2009)

[25] Sade M., Baruj A., Troiani H.E.: fcc/hcp martensitic transformation temperatures and thermal cycling evolution in Fe-Mn-Cr alloys. Proc. Int. Conf. New Developments on Metallurgy and Applications of High Strength Steels, Buenos Aires, Argentina (2008) 1183-1191

[26] Guerrero L.M., La Roca P., Malamud F., Baruj A., Sade M.: Composition effects on the fcc-hcp martensitic transformation and on the magnetic ordering of the fcc structure in Fe-Mn-Cr alloys, Mater. Des. 116 (2017) 127–135.

[27] Baruj A., Cotes S., Sade M., Fernández Guillermet A.: Coupling binary and ternary information in assessing the fcc/hcp relative phase stability and martensitic transformation in Fe-Mn-Co and Fe-Mn-Si alloys, J. Phys. IV France 5 (1995) (C8-373-378)

[28] Cotes S., Fernández Guillermet A., Sade M.: Phase stability and fcc/hcp martensitic transformation in Fe-Mn-Si alloys. Part I. Experimental study and systematics of the Ms and As temperatures, J. Alloys Compd. 278 (1998) 231–238

[29] Cotes S.M., Fernández Guillermet A., Sade M.: Fcc/hcp martensitic transformation in the Fe-Mn system: part II. Driving force and thermodynamics of the nucleation process, Metall. Mater. Trans. A 35A (2004) 83–91

[30] Cotes S., Sade M, and Fernández Guillermet A.: Fcc/hcp Martensitic Transformation in the Fe-Mn System: Experimental Study and Thermodynamic Analysis of Phase Stabilities. Met. Trans. A., Volume 26A (1995) 1957-1969

[31] Khomenko O.A., Khil'kevich I.F., Zvigintseva G.Y.: Influence of a third component on the Néel point of iron-manganese invars, Fiz. Met. Metalloved. 37 (1974) 1325–1326

[32] Zhang Y.S., Lu X., Tian X., Quin Z.: Compositional dependence of the Néel transition, structural stability, magnetic properties and electrical resistivity in Fe-Mn-Al-Cr-Si alloys, Mater. Sci. Eng. A 334 (2002) 19–27

[33] Huang W.: An assessment of the Fe-Mn system, Calphad 13 (1989) 243–252

[34] Nyilas A., Weiss K., Grikurov G., Zoidze N.: Tensile, fracture, and fatigue crack growth rate behavior of high manganese steels, AIP Conf. Proc. 824 (I) (2006) 130–137

[35] Marinelli P., Sade M., Baruj A., Guillermet A.F.: Lattice parameters of metastable structures in quenched Fe-Mn alloys. Part. I. Experimental techniques, bcc and fcc phases, Z. Metallkd. 91 (2000) 957–962

[36] Fu H., Xu S., Zhao H., Dong H., Xie J.: Cyclic stress-strain response of directionally solidified polycrystalline Cu-Al-Ni shape memory alloys, J. Alloys Compd. 714 (2017) 154–159

[37] Sade M., La Roca P., De Castro Bubani F., Lovey F.C., Torra V., Yawny A., Pseudoelastic cycling between austenite, 18R and 6R phases in CuAlBe single crystals, Mater. Today Proc. 2 (Suppl. 3) (2015) S719–S722

[38] Zotov N., Pfund M., Polatidis E., Mark A.F., Mittemeijer E.J.: Change of transformation mechanism during pseudoelastic cycling of NiTi shape memory alloys, Mater. Sci. Eng. A 682 (2017) 178–191

[39] Isola L., La Roca P., Sobrero C., Fuster V., Vermaut P., Malarría J.: Study of the loadbiased martensitic transformation strain and stability of Ni50 − x-Ti-Cox strips obtained by twin-roll and standard casting techniques, Mater. Des. 107 (2016) 511–519

[40] Omori T., Ando K., Okano M., Xu X., Tanaka Y., Ohnuma I., Kainuma R., Ishida K.: Superelastic effect in polycrystalline ferrous alloys, Science 333 (2011) 68–71

[41] La Roca P., Baruj A., Sobrero C.E., Malarria J.A., Sade M., Nanoprecipitation effects on phase stability of Fe-Mn-Al-Ni alloys", Journal of alloys and compounds, Vol. 708, (2017), Pages 422-427.

[42] Rawers J.C.: Alloying effects on the microstructure and phase stability of Fe–Cr–Mn steels, J. Mater. Sci. 43 (2008) 3618–3624

[43] Reeh S., Kasprzak M., Klusmann C.D., Stalf F., Music D., Ekholm M., Abrikosov I.A., Schneider J.M.: Elastic properties of fcc Fe–Mn–X (X= Cr, Co, Ni, Cu) alloys studied by the combinatorial thin film approach and ab initio calculations, J. Phys. Condens. Matter 25 (2013), 245401

[44] Tamarat K., Stambouli V., Bouraoui T., Dubois B.: Structural study of Fe-Mn-Si and Fe-Mn-Cr shape memory steels, J. Phys. IV 01 (1991) (C4-347–C4-353)

[45] Malamud F., Guerrero L.M., La Roca P., Sade M., Baruj A.: Role of Mn and Cr on structural parameters and strain energy during FCC-HCP martensitic transformation in Fe-Mn-Cr shape memory alloys, Mater. Des. 139 (2018) 314-323

[46] Marinelli P., Baruj A., Guillermet A.F., Sade M.: Lattice parameters of metastable structures in quenched Fe-Mn alloys. Part II: hcp phase, Z. Met. 92 (2001) 489–493

[47] Marinelli P., Sade M., Fernández Guillermet A.: On the structural changes accompanying the fcc/hcp martensitic transformation in Fe–Mn–Co alloys, Scr. Mater. 46 (2002) 805–810

[48] Malamud F., Castro F., Guerrero L.M., La Roca P., Sade M., and Baruj A.: High-precision face-centered cubic-heagonal close-packed volume-change determination in high-Mn steels by X-ray diffraction data refinements, J. Appl. Cryst. (2020) 53, 34-44

[49] Kaufman L. and Cohen M.: Thermodynamics and kinetics of martensitic transformations. Prog. Met. Phys. 1958. pp. 165-246

[50] Guerrero L.M., La Roca P., Malamud F., Baruj A., Sade M.: Experimental determination of the driving force of the fcc-hcp martensitic transformation and the stacking fault energy in high-Mn Fe-Mn-Cr steels, J. Alloy Compd. Vol. 797 (2019) 237-245

[51] Martin J.W., Doherty R.D., Cantor B.: Stability Of Microstructure In Metallic Systems, Cambridge Solid State Science Series, 1997

[52] Nakano J., Jacques P.J.: Effects of the thermodynamic parameters of the hcp phase on the stacking fault energy calculations in the Fe-Mn and Fe-Mn-C systems. CALPHAD 34 (2010) 167 – 175

[53] Lee Y.K. and Choi C.S.: Driving Force for ϒ→ε Martensitic Transformation and Stacking Fault: Energy of ϒ in Fe-Mn Binary System. Metall. Mater. Trans. A Vol. 31A, (2000) 355-360

[54] Baruj, A., Fernández Guillermet, A., Sade, M.: Effects of thermal cycling and plastic deformation upon the Gibbs energy barriers to martensitic transformation in Fe-Mn and Fe-Mn-Co alloys. Mat. Sci. Eng. A 273-275(1999) 507-511

[55] Olson G. B., Cohen M.: A General Mechanism of Martensitic Nucleation Part I. General Concepts and the FCC→ HCP Transformation. Metall. Trans. A Vol. 7A, (1976) 1897-1904

[56] Ghosh G. and Olson G.B.: Computational Thermodynamics and the Kinetics of Martensitic Transformation. J. Phase Equilib. Vol. 22 No. 3 2001

[57] Palumbo M.: Thermodynamics of martensitic transformations in the framework of the CALPHAD approach. CALPHAD 32 (2008) 693-708

[58] Pisarik S.T., Aken D.C.V.: Thermodynamic driving force of the γ → ε transformation and resulting Ms temperature in high-Mn steels, Metall. Mater. Trans. A 47 (2016) 1009–1018

[59] Mertinger V., Benke M., Nagy E., Pataki T.: Reversible characteristics and cycling effects of the martensitic transformations in Fe-Mn-Cr TWIP/TRIP steels, J. Mater. Eng. Perform. 23 (2014) 2347–2350.

[60] Baruj A., Cotes S., Sade M. and Fernández Guillermet A.: Effects of thermal cycling on the fcc/hcp martensitic transformation temperatures in Fe-Mn Alloys. Z. Metallkd. 87 (1996) 10

[61] Baruj, A.; Troiani, H.E.; Sade, M.; Fernández Guillermet, A.: Effects of thermal cycling on the fcc/hcp martensitic transformation temperatures in the Fe-Mn system: Part II. TEM study of the microstructural changes. Philos. Mag. A. 80 (2000) 2537-2548.

[62] Krishnan R.V., Delaey L., Tas H., Warlimont H.: Thermoplasticity, pseudoelasticity and the memory effects associated with martensitic transformations – Part 2 The macroscopic mechanical behavior. J Mater Sci 9(9) 1536-1544 (1974)

[63] Baruj A., Bertolino G., Troiani H.E, Temperature dependence of critical stress and pseudoelasticity in Fe-Mn-Si-Cr pre-rolled alloy, J. Alloy Compd 502 (2010) 54-58

[64] Otsuka H., Nakajima K., Maruyama T.: Superelastic Behavior of Fe–Mn–Si–Cr Shape Memory Alloy Coil. Mater. Trans JIM 41 (2000) 547-549

[65] Matsumura O., Sumi T., Tamura N., Sato K., Furukawa T., Otsukka H.: Pseudoelasticity in an Fe–28Mn–6Si–5Cr shape memory alloy. Mater. Sci. Eng. A 279 (2000) 201-206

[66] Sawaguchi T., Kikuchi T., Kajiwara S.: The pseudoelastic behavior of Fe–Mn–Si-based shape memory alloys containing Nb and C. Smart Mater Struct 14 (2005) S317-S322

[67] Druker A., Vermaut P., Malarría J.: The shape recovery conditions for Fe-Mn-Si alloys: An interplay between martensitic transformation and plasticity, Mater. Charact. 139 (2018) 319-327

[68] Druker A., La Roca P., Vermaut P., Ochin P., Malarría J.: Microstructure and shape memory properties of Fe-15Mn-5Si-9Cr-5Ni melt spun ribbons, Mater. Sci. Eng. A vol. 556 (2012) 936-945

[69] Druker A., La Roca P., Vermaut P., Ochin P., Malarría J.: The shape memory effect in melt spun Fe-15Mn-5Si-9Cr-5Ni alloys, Mater. Sci. Forum Vols. 738-739 (2013) pp 247-251

[70] Nevin Balo S., Yakuphanoglu F.: The effects of Cr on isothermal oxidation behavior of Fe-30Mn-6Si alloy, Thermochim. Acta 560 (2013) 43-46

Figures

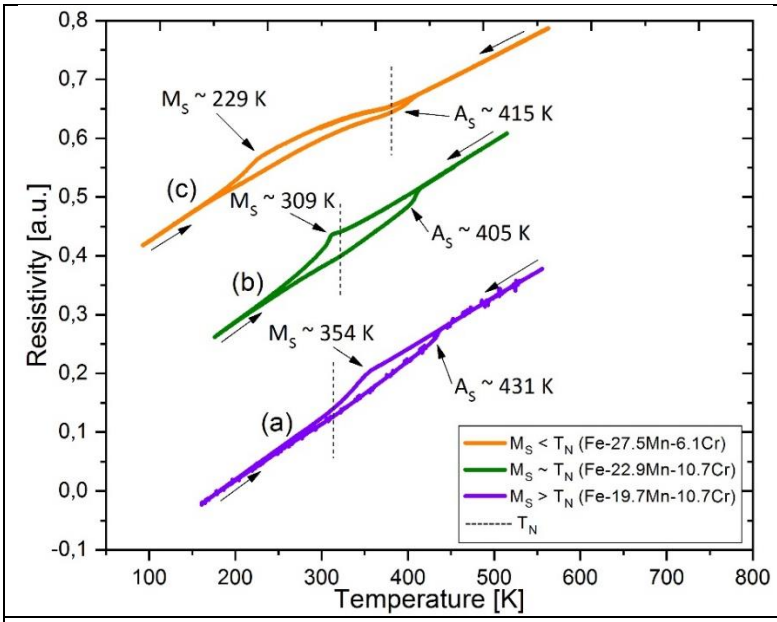

Figure 1. Electrical resistivity vs. temperature measurements for Fe-Mn-Cr alloys [26]. The short vertical dotted lines mark the para-antiferromagnetic transition temperature (T_N) of each alloy. Curve (a) corresponds to the case where $M_S > T_N$, curve (b) shows the intermediate behavior, and curve (c) shows the case where $M_S < T_N$. M_S and A_S are also indicated in curves (a), (b) and (c). Reprinted from Ref. [26], Copyright (2017), with permission from Elsevier.

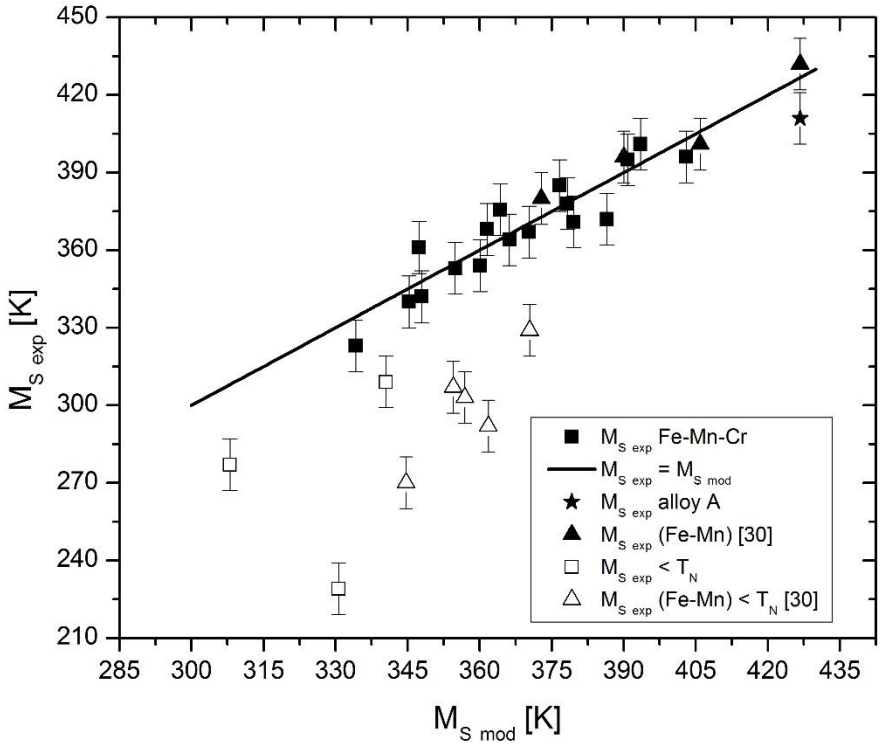

Figure 2. Experimentally obtained M_S temperatures vs. modeled values. Data for Fe-Mn-Cr alloys obtained by [26] and Fe-Mn alloys reported by [30]. The empty symbols represent data where $M_S<T_N$. The solid line represents Eq. 1 results. References in the inset correspond to the present manuscript. Reprinted from Ref. [26], Copyright (2017), with permission from Elsevier.

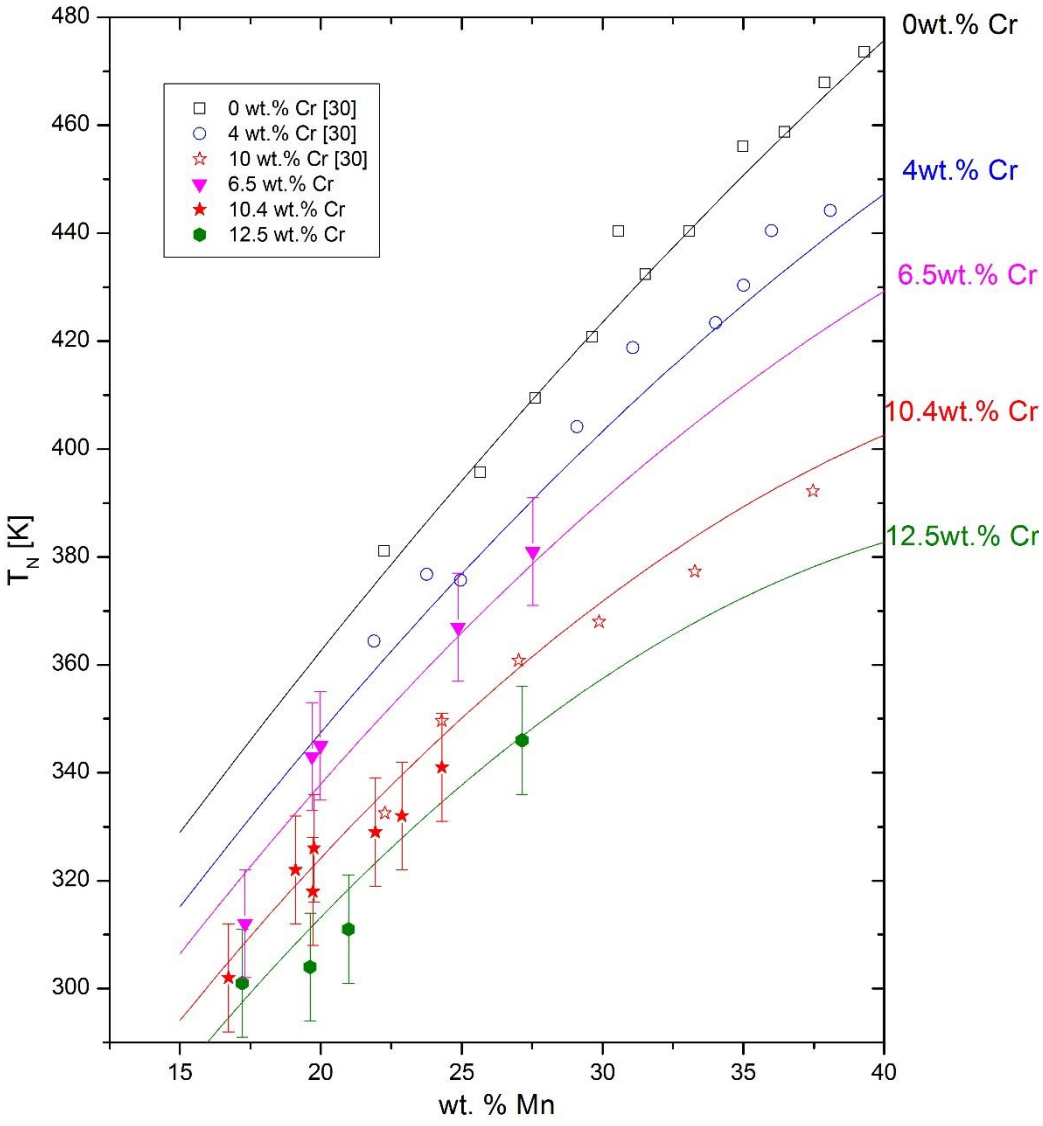

Figure 3. T_N vs. Mn content for different amounts of Cr. Data reported by references [26,30] are included. Curves correspond to the phenomenological model (Eq. 2). References in the inset correspond to the present manuscript. Reprinted from Ref. [26], Copyright (2017), with permission from Elsevier.

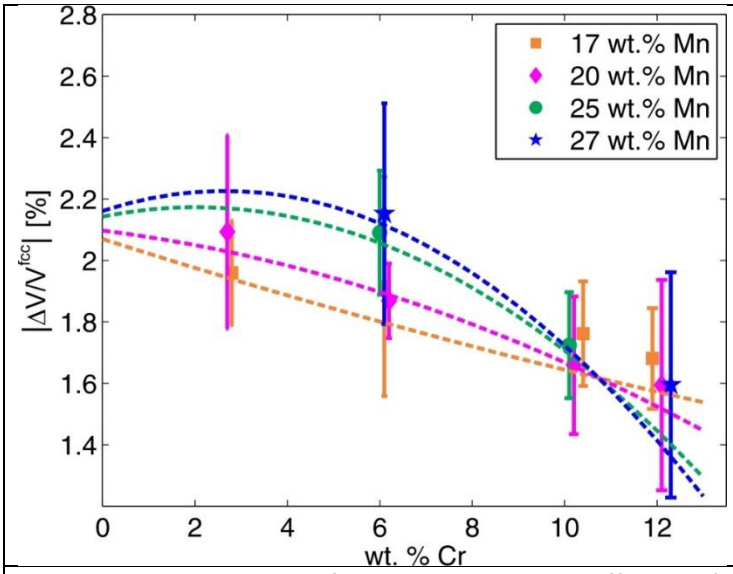

Figure 4. Absolute value of the relative volume difference (in percent) between fcc and hcp phases as a function of Cr content for different amounts of Mn. Dotted lines correspond to calculated values with the phenomenological model presented in Ref. [45] and solid dots correspond to experimental results. In all cases the hcp volume per atom is smaller than the corresponding one to the fcc structure. Reprinted from Ref. [45], Copyright (2018), with permission from Elsevier.

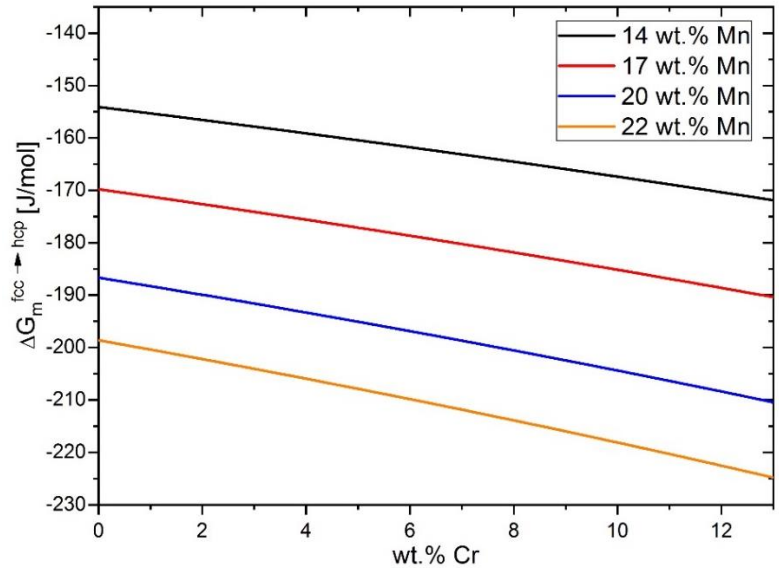

Figure 5. Curves calculated from experimental driving forces values of the fcc-hcp martensitic transformation at M_S as function of Cr content from Ref. [50]. The 0 wt.% Cr curve corresponds to an extrapolation made from the measured values. $\Delta G_m^{fcc \rightarrow hcp}$ is defined as $\left(G_m^{hcp} - G_m^{fcc}\right)$. Reprinted from Ref. [50], Copyright (2019), with permission from Elsevier.

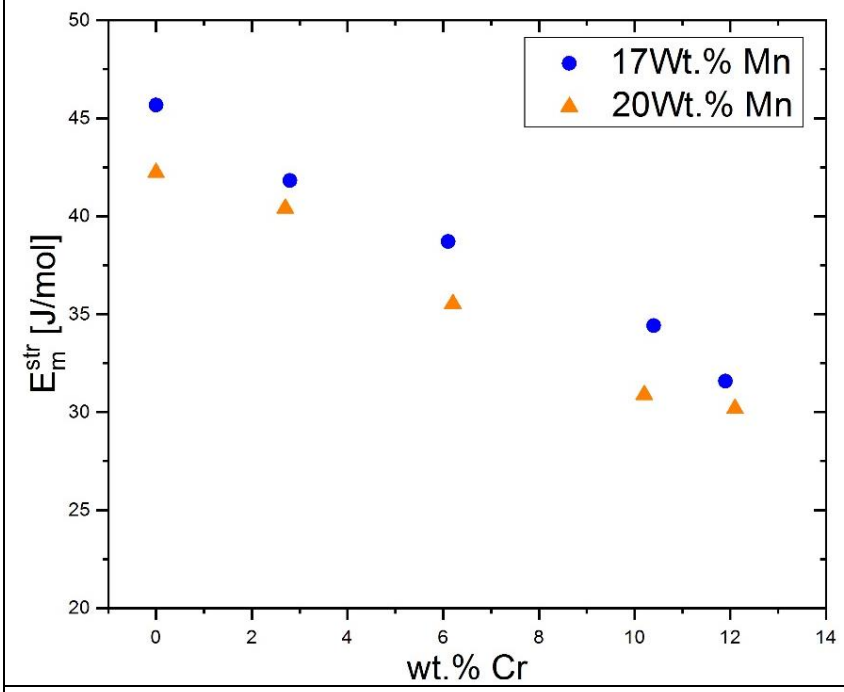

Figure 6. Calculated strain energy of Fe-Mn-Cr alloys as a function of the Cr content at different Mn contents. Experimental plotted data obtained from Ref. [45].

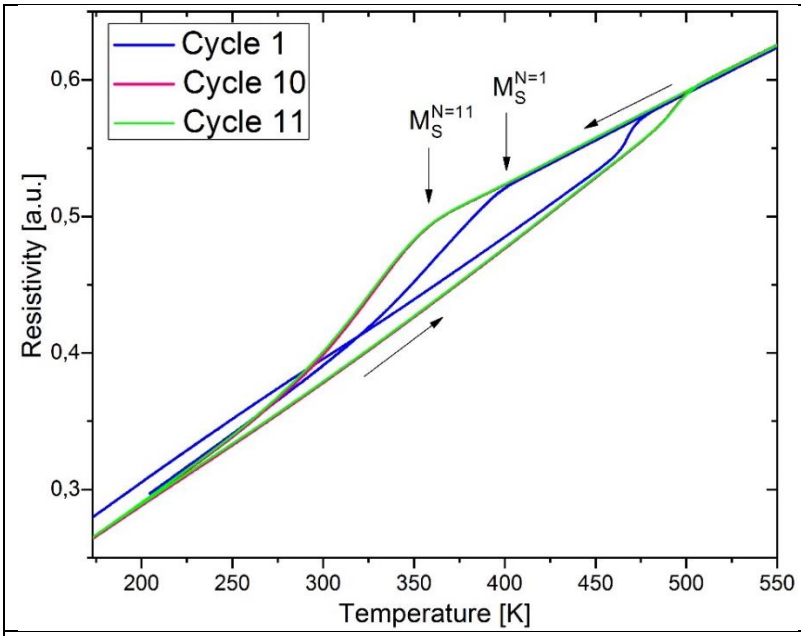

Figure 7. Effect of cycling in martensitic transformation temperatures for alloy A, from electrical resistivity measurements. The figure shows cycles 1, 10 and 11. $M_S^{N=1}$ correspond to the first cycle and $M_S^{N=11}$ correspond to the last two cycles. Cycles 10 and 11 exactly overlap.

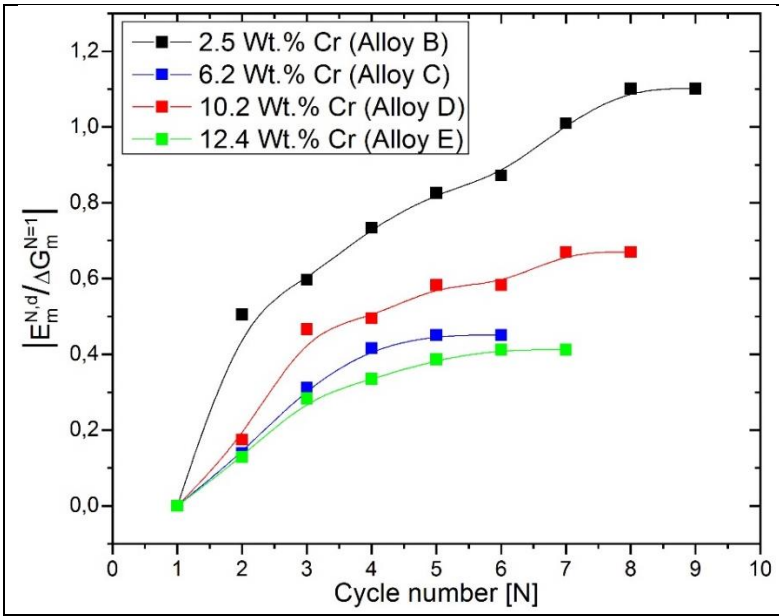

Figure 8. Effect of thermal cycling on the barrier that oppose the martensitic transformation, for alloys with 20 Wt.% Mn and different amounts of Cr. According to the text $E_m^{N,d} > 0$ and $\Delta G_m^{N=1} < 0$.

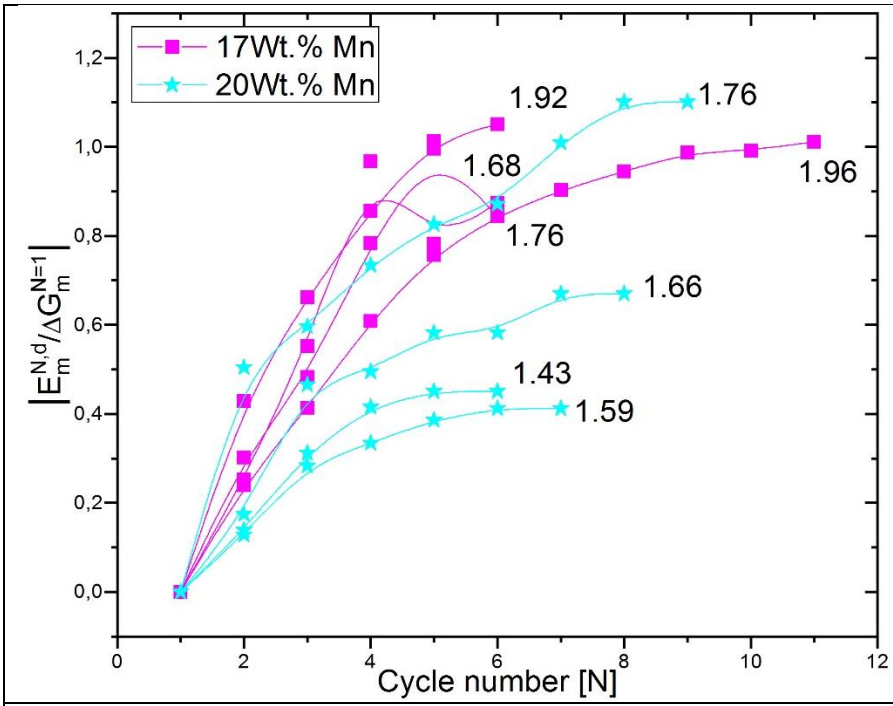

Figure 9. Effect of thermal cycling on the barrier that oppose the martensitic transformation, for alloys with 17 Wt.% Mn and 20 Wt.% Mn, with different amounts of Cr. Number close to each curve is the volume change related to the fcc-hcp martensitic transformation. According to the text $E_m^{N,d} > 0$ and $\Delta G_m^{N=1} < 0$.

Table:

Table 1. Chemical composition of the used alloys, determined by neutron activation technique, measured martensitic transformation temperature (M_S), magnetic ordering temperature of the fcc structure (T_N), driving force of the fcc-hcp martensitic transformation (ΔG_m), and the energetic barrier increment due to the dislocation density $\left(E_m^{N,d}\right)$. The superscript *N,d* in the $\left(E_m^{N,d}\right)$ indicates the contribution of dislocations to the barrier energy for cycle N. $E_m^{N,d}$ in the last column corresponds to the last performed thermal cycle which is 11, 9, 6, 8 and 7 for samples A, B, C, D and E, respectively.

Alloys	**Wt.% Fe**	**Wt.% Mn**	**Wt.% Cr**	**$M_S^{N=1}$ [K]**	**T_N [K]**	**$\Delta G_m^{N=1}$ [J/mol]**	**$E_m^{N,d}$ [J/mol]**
A	79.3	17.9	2.8	396	330	-223	226
B	76.8	20.7	2.5	395	369	-124	136
C	74.1	19.7	6.2	378	345	-164	74
D	70.0	19.8	10.2	368	326	-208	139
E	66.6	21.0	12.4	340	311	-245	101